Nov 7th, 12:00 AM - Nov 8th, 12:00 AM

Investigation on Shear Capacity for Screw Connections of Cold-Formed Steel Framed Shear Walls with Steel Sheathing

Ruoqiang Feng

Ying Ma

Wei-Wen Yu International Specialty Conference on Cold-Formed Steel Structures
St. Louis, Missouri, U.S.A., November 7 & 8, 2018

Investigation on shear capacity for screw connections of cold-formed steel framed shear walls with steel sheathing

Feng Ruoqiang[1], Ma Ying, Zhu Baochen

ABSTRACT

Experimental and numerical investigations were carried out to learn the shear capacities for screw connections of cold-formed steel framed shear walls with steel sheets for the base layer combined with gypsum wallboards for the face layer. The design methods of test specimens, the loading equipment and the data processing method were introduced. According the phenomenon of tests for multiple self-drilled screw connections, the loading-deformation curves, shear capacity and failure modes were testified. The influence of end distance of screw, edge distance of screw, diameter of screw, spacing of screw, thickness of steel sheets, thickness of gypsum wallboards, thickness of studs on shear behavior for connections were investigated. The finite element software ABAQUS was used to simulate the shear behavior of screw connections. A comparison between the numerical simulations and the test results showed a good agreement. This study can be applied to numerical simulations of seismic behavior of steel sheathed cold-formed steel framed shear walls.

Keywords: CFS framed shear wall, Screw connection, Steel sheathing, Finite element analysis

1. Introduction

Cold-formed steel structures have been widely used in residential and small commercial buildings in the USA, Japan, and Australia in past years because of their lightweight, ease of installation, and environmental characteristics [1]. Cold-formed steel framed shear walls, attached with oriented-strand board, gypsum board or cement board sheathing normally, is an important component in CFS structure, which resist the horizontal loads such as earthquake loads and wind loads. In recent years, steel sheathings on CFS shear walls have been used

[1] Professor, Southeast University, Nanjing, Jiangsu, China, hitfeng@163.com

to achieve higher shear resistance in extreme loading incidents. However, It was observed that the fire resistance time of the normal steel structure without any protection ranged from 10 to 22 min, which was difficult to achieve a fire rating of more than 120 min for load- bearing walls under service load in mid-rise buildings [2]. Chen W and Ye et al [3] reported that the fire resistant performance of CFS wall systems mainly depended on the protection of wall panels and the performance of fire-resistant gypsum plasterboard was considerably good. Consequently, the CFS shear wall sheathed with steel sheets for the base layer combined with gypsum wallboards for the face layer have been proposed and experimented.

Since the screw connections have the important influence on the shear performance of CFS walls [4-5], and the screw connection between the CFS studs and sheathings was obviously hinged. Therefore, to evaluate the shear capacities of the steel sheathing screw connections in CFS walls, Mohebbi and Mirghaderi [6] tested three sets of lap-joint specimens and obtained the shear performance and failure modes of those connections such as tilting of screws. However, the flanges of studs can limit the out-of-plane curling in tests of connections, which would lead to more accurate results [7]. Fiorinoa and Della [8] used a typical test setup to conduct tests on screw connections between cold-formed steel stud and wood- or gypsum-based panels and found the effect of sheathing orientation. Nithyadharan and Kalyanaraman [9], who found that the screws in a wall panel under in-plane shear actually experienced shear essentially parallel to the sheathing edge. And designed a new test setup in which the load direction was parallel to the free edge of sheathing, to examine the shear response of the connections with calcium silicate boards. In order to predict the load–displacement curves and the failure modes of screws connections without test, a few computational modeling of cold-formed steel screwed connections were conducted by Wei Lu and L.Fan et al [10-12].

In this paper, the experimental and numerical study were conducted to investigate the shear capacity of screw connections in CFS shear walls sheathed with steel sheet for the base layer combined with gypsum wallboards for the face layer. The failure mechanism and shear capacity of specimens with different specifications under monotonic tension were obtained. The finite element software ABAQUS was used to simulate the shear behavior of screw connections. The numerical simulations showed an agreement with the test results.

2. Experiment details

2.1 Test specimens

34 sets of specimens for screw connections of cold-formed steel framed shear walls with steel sheets as the base layer combined with gypsum wallboards as the face layer were conducted. To explore the effects of diameter of screw (4.2 mm, 4.8 mm and 5.5 mm), thickness of steel sheets (0.8 mm and 1.2 mm), thickness of gypsum wallboards (12 mm and 15 mm), and thickness of CFS studs (0.9 mm, 1.2 mm and 2.5 mm) on shear behavior for connections, so the sheathings, CFS studs and screws of different specifications were used in specimens. Two different test setups having three screw spacing (100 mm, 150 mm and 200 mm) were tested under monotonic tension to investigate the influence of the end distance of screw (15 mm, 20 mm and 25 mm) and edge distance of screw (15 mm, 20 mm and 25 mm). The sectional types of CFS studs are shown in Fig. 1 and Table 1. The different test specimens in the program were summarized in Table 2 and the series labels for each specimen are defined in Fig. 2.

Table 1

Specifications of CFS studs

Identifier	H(mm)	B(mm)	A (mm)	T (mm)
C0.9	89	50	13	0.9
C1.2	140	50	13	1.2
C2.5	140	50	13	2.5

H is the width of webs; B is the width of flanges; A is the width of lips; T is the thickness of studs.

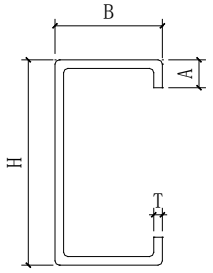

Fig. 1 The sectional type of studs

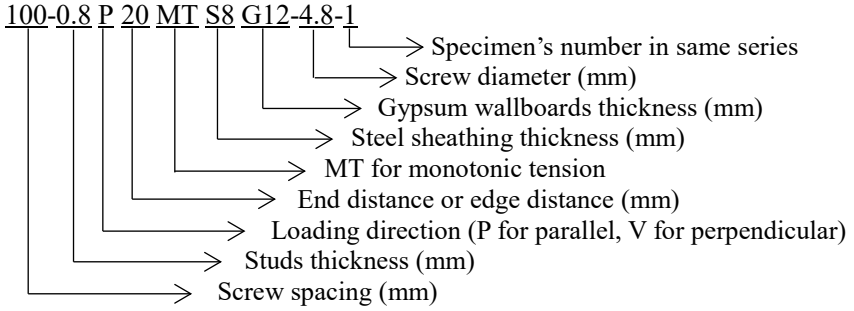

Fig. 2 Definition of the series labels

Table 2

Test results of the screw connections

Specimens		δ_y (mm)	F_y (N)	δ_m (mm)	F_m (N)	δ_u (mm)	F_u (N)	μ	M	F_{avg} (N)
100-1.2P 25MTS8 G12-4.8	1	4.93	3509.58	7.50	4140.41	12.49	3519.35	2.53	A	3964.15
	2	4.38	3222.57	6.78	3787.89	10.22	3219.70	2.34	A	
150-1.2P 25MTS8 G12-4.8	1	5.71	3823.26	8.36	4364.22	10.12	3709.58	1.77	A	4222.45
	2	4.81	3491.61	7.31	4080.69	9.11	3468.59	1.90	A	
200-1.2P 25MTS8 G12-4.8	1	4.87	3364.05	7.36	4064.46	8.96	3454.79	1.84	A	4018.94
	2	4.73	3398.84	7.25	3973.43	8.92	3377.41	1.89	A	
100-1.2V 25MTS8 G12-4.8	1	4.67	2991.81	7.03	3533.35	9.29	3003.35	1.99	A	3540.89
	2	4.94	3115.89	7.58	3548.43	10.90	3016.16	2.20	A	
150-1.2V 25MTS8 G12-4.8	1	5.56	3024.28	7.71	3471.89	8.79	2951.11	1.58	A	3706.71
	2	6.83	3543.79	8.55	3941.54	10.10	3350.31	1.48	A	
200-1.2V 25MTS8 G12-4.8	1	4.39	2868.89	7.03	3340.86	8.00	2839.73	1.82	A	3506.10
	2	6.02	3118.21	8.34	3671.35	12.22	3120.64	2.03	A	
150-0.9P 25MTS8 G12-4.8	1	5.25	3724.69	6.98	4069.09	8.85	3458.73	1.69	E	4026.77
	2	7.03	3420.29	10.13	3984.44	12.62	3386.78	1.79	E	
150-2.5P 25MTS8 G12-4.8	1	4.53	3746.14	6.76	4458.15	9.11	3789.42	1.75	B	4421.33
	2	3.71	3829.05	5.15	4384.51	7.56	3726.83	2.04	B	
150-1.2P 15MTS8 G12-4.8	1	4.69	3394.78	7.18	3990.24	9.82	3391.70	2.10	A	3902.11
	2	4.54	3158.22	7.84	3813.98	9.26	3241.88	2.04	A	
150-1.2P 20MTS8 G12-4.8	1	5.02	3677.72	8.11	4347.40	9.28	3695.29	1.85	A	4364.07
	2	5.16	3715.41	8.00	4380.74	9.87	3723.63	1.91	A	
150-1.2V 15MTS8 G12-4.8	1	5.60	3342.02	7.42	3863.84	9.09	3284.27	1.62	A	4033.73
	2	5.09	3539.15	7.61	4203.61	9.55	3573.07	1.88	A	
150-1.2V 20MTS8 G12-4.8	1	6.51	3148.36	8.95	3780.35	13.61	3213.30	2.09	A	3589.59
	2	5.46	2894.40	7.83	3398.84	8.51	2889.01	1.56	A	

150-1.2P	1	4.81	3226.63	7.31	4080.69	9.11	3468.59	1.90	A	
25MTS8										4107.65
G12-4.2	2	4.63	3543.21	6.86	4134.61	9.00	3514.42	1.94	A	
150-1.2P	1	5.61	3954.29	8.30	4543.96	12.45	3862.36	2.22	A	
25MTS8										4480.76
G12-5.5	2	5.83	3826.16	8.65	4417.56	11.22	3754.93	1.93	A	
150-1.2P	1	4.89	3551.33	7.59	4110.26	9.11	3468.59	1.86	A	
25MTS8										4269.42
G15-4.8	2	4.95	3827.31	7.00	4428.58	9.89	3764.29	2.00	A	
150-1.2P	1	5.63	4909.82	10.58	5768.51	11.11	4903.24	1.97	D	
25MTS12										5611.96
G12-4.8	2	5.21	4750.95	9.72	5455.42	11.13	4637.10	2.14	D	
150-2.5V	1	4.94	3619.16	6.80	4093.45	7.98	3479.43	1.62	C	
25MTS8										4109.68
G12-4.8	2	4.87	3772.23	6.27	4125.92	6.75	3507.03	1.38	C	

F_y and δ_y are the yield strength and its relative displacement, F_m is the peak load, δ_m is the relative displacement corresponding to F_m, F_u equals $0.85F_m$ beyond the peak load, δ_u is the relative displacement corresponding to F_u, μ is the ductility coefficient, M means the failure mode in Table 3 and F_{avg} is the average value of the same set of specimens.

2.2 Test setup and procedure

Depending on whether the influence of end distance or edge distance of screws on shear performance of screws connection was investigated, two test setups were used in the experimental program. Fig. 3 shows the setup was used to testing the influence of edge distance of screws on shear performance of screws connection, which achieve the screw shearing which the shearing direction parallel to the nearest free edge of the sheathing. Two pairs of CFS studs were back to back bolted to each other with the 6 mm steel plates gripping by loading jaws, using 14 mm bolts. Four 200 mm wide sheathings composed of steel sheets for the base layer combined with gypsum wallboards for the face layer were

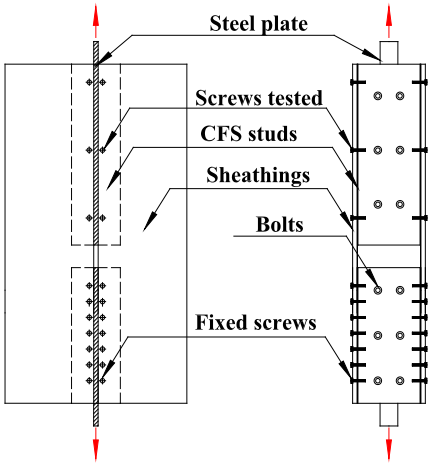

Fig. 3 Test setup of connections achieving shear in screws parallel to edge

connected to the flanges of top studs by three screws and the bottom studs by seven screws at desired edge distance from free edge of the board, to ensure failure in the screws at the top connection.

Fig. 4 shows the setup was used to testing the influence of the end distance of screws on shear performance of screws connection, which achieve the screw shearing which the shearing direction perpendicular to the nearest free edge of the sheathing. CFS studs were bolted to the 6 mm steel plates on the inner side and the steel T-sections gripped by loading jaws on outer side. Sheathings were connected to the flanges of top stud by three screws at desired edge distance from the free edge of the board and were fixed to the bottom stud by seven screws to avoid failure at this end.

A 100 kN servocontrolled testing machine system was used to apply axially forces to the specimens using the displacement-controlled mode at a loading velocity of 0.03 mm/s. The load and displacement of specimens were measured and recorded by the servocontrolled testing machine system.

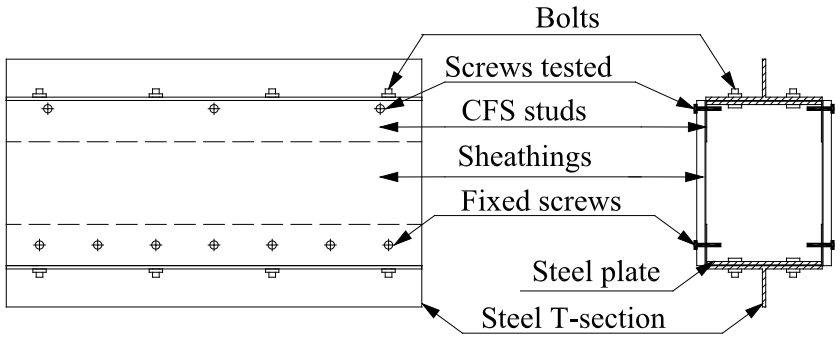

Fig. 4 Test setup of connections achieving shear in screws perpendicular to edge

3. Experimental results

3.1. Failure mechanisms

The following destruction phenomena shown in Fig. 5 were observed in the test: tilting of screws (T), pullout of the screw (P), Screw shearing (S), bearing of gypsum board (BG), bearing of steel sheathing (BS), bearing of studs (BT), tearing of steel sheathing (TS) and cracking of gypsum board (C). According to the combination of phenomena, several failure modes of connections are summarized in Table 3.

In the tension tests of specimens which achieve screw shearing which the shearing direction parallel to the nearest free edge of the sheathing, the bearing in the gypsum wallboards increased gradually with the displacement applied. When the load approached the peak value, cracks at the edge of gypsum wallboards appeared and developed with increased of displacement. The failure of specimens was resulted from pullout of screw with 0.8 mm steel sheathing and screw shearing with 1.2 mm steel sheathing. Bearing of 1.2 mm steel sheathing and tearing of 0.8 steel sheathing were observed after removing gypsum wallboards. Screws were tilted in tests with 0.9 mm and 1.2 mm studs and bearing of studs appeared only in tests with 0.9 mm studs. The general failure characteristics of the specimens were nearly the same with different edge distances and spacing of screws.

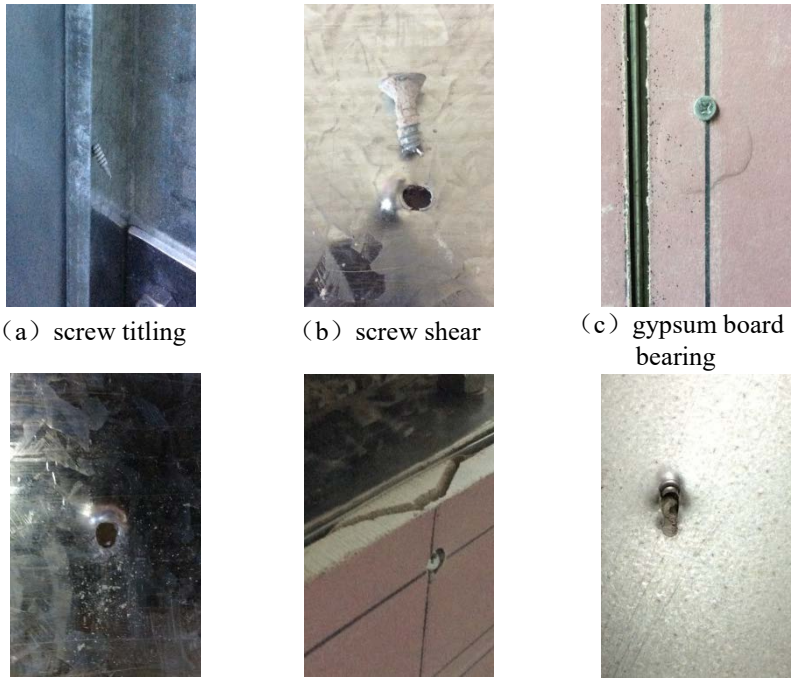

（a）screw titling　（b）screw shear　（c）gypsum board bearing

（d）stud bearing　（e）gypsum board cracking　（f）steel sheathing bearing and tearing

Fig. 5 Destruction phenomena of screw connections

Table 3
Failure modes of specimens

Failure modes	Destruction phenomena
A	T+BG+BS+TS+C+P
B	T+BS+TS+C+P
C	T+S+BG+BS+BT+P
D	T+BG+BS+BT+TS+C
E	T+BS+BT+TS+C+P

T is screw tilting, P is screw pull-out, S is screw shear, BG is gypsum board bearing, BS is steel sheathing bearing, BT is stud bearing, TS is steel sheathing tearing and C is gypsum board cracking.

Compared to tests which achieve shear in screws parallel to the nearest free edge of the sheathing, phenomena of tests which achieve shear in screws perpendicular to the nearest free edge of the sheathing was similar expect the position and shape of cracks at the edge of gypsum wallboards since V-shaped cracking along the sheathing thickness were observed. The open-end width of the V-shaped cracking increased with the end distance of screws.

3.2. Load-deformation behavior

The load–deformation curves of specimens with different edge distance and end distance of specimens by tension is shown in Fig. 6. The initial part of the curve is approximately linear while the curve becomes non-linear at around 30% of the ultimate load. A gradual reduction of the load appears after the loading reaches the ultimate value, showing ductile failure. Only the loading-displacement curve of specimens with 1.2 mm steel sheathing shows the characteristics of shear failure since the load diminish rapidly after reaching the maxima, as shown in Fig. 12(d) .

Six parameters were used to characterize the loading-displacement behavior of screws, where F_m is the peak load, δ_m is the relative displacement corresponding to F_m, F_y and δ_y are the yield strength and its relative displacement, respectively, based on the equivalent elasto-plastic energy absorption [13], F_u equals $0.85F_m$ beyond the peak load, δ_u is the relative displacement corresponding to F_u; and the ductility coefficient μ is δ_u divided by δ_y. Table 2 summarized these parameters and failure modes of all sets of specimens.

3.3 Parameter analysis

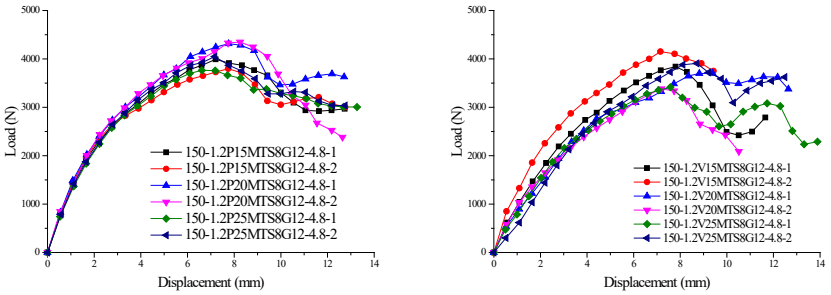

(a) Edge distance (b) End distance

Fig. 6 The load–deformation curves of specimens with different edge distance and end distance

3.3.1 Effect of edge distance, end distance and spacing

The average peak strength of the screw connections for different edge distance, end distance and spacing have been plotted in Fig. 7. It can be seen from the Fig. 7(a-c), there was tiny fluctuations in the all curves, which indicated that there is little effect of end distance over 15 mm, edge distance over 15 mm and spacing over 100 mm on shear capacities of the connections. A minor influence on shear capacity owing to the failure area of steel sheathings center on screws was small compared with end distance, edge distance and spacing.

3.3.2 Effect of sheathing thickness

According to Table 2, as steel sheathing thickness increased from 0.8 mm to 1.2 mm, the average peak load improved by 32.9% since the failure modes of connections changed from screw tilting to screw shear with increase of steel sheathing thickness. The shear capacities of connections had little correlation with thickness of gypsum wallboards, owing to the gypsum wallboards had cracked already before the load reached the peak value.

3.3.3 Effect of stud thickness

As shown in Fig. 7(d), there was gradual rise of peak load and the upward trend slowed down with increase of stud thickness. The reason for this behavior is that the increase of stud thickness improved the restraint of screw tilting, which was related to shear capacity of connections. When the stud thickness is big enough that the screw would not tilt, the shear capacity would depend on steel sheathings instead of stud thickness.

3.3.4 Effect of screw diameter

The increase in the screw diameter produced a gradual increase of the shear capacities of the connections shown in Table 2, because compression area of the sheathings surrounding screws became larger with the increase of screw

diameter.

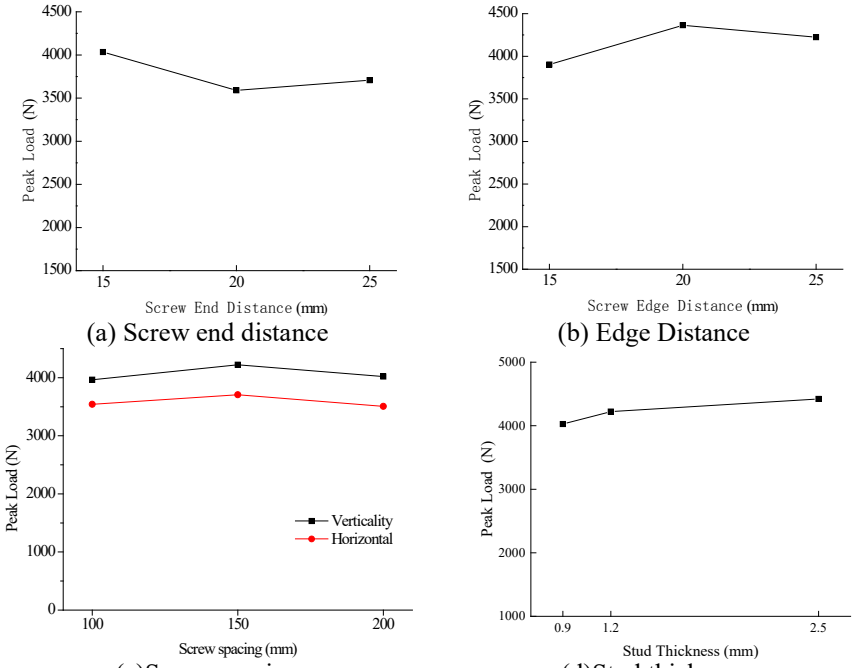

(a) Screw end distance (b) Edge Distance

(c)Screw spacing (d)Stud thickness

Fig. 7 The average peak strength of the screw connections

4. Numerical modeling

4.1 Finite element modeling of screw connections

ABAQUS/Standard 15[14] was used to establish the finite element models of screw connections with three-dimensional solid elements C3D8R. Considering the symmetry of specimens and loads, a quarter of the test specimen was modeled simplistically as shown in Fig. 8. Gypsum wallboards were not considered in the model owing to the fact that gypsum wallboards had little influence on the shear capacities of screw connections. Only two threads of screw were created and the screw holes in steel sheathings and studs were cylinders, as shown in Fig. 9. The frictionless hard contact with finite sliding was used in the contact pairs between the steel sheathing and the stud, between the steel sheathing and the screw shank, between the stud and the screw shank, between the steel sheathing and the screw thread, and between the thicker plate

and the screw threads.

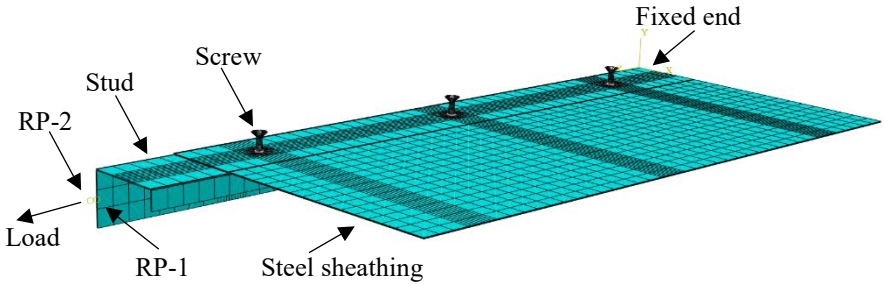

Fig. 8 Finite element model

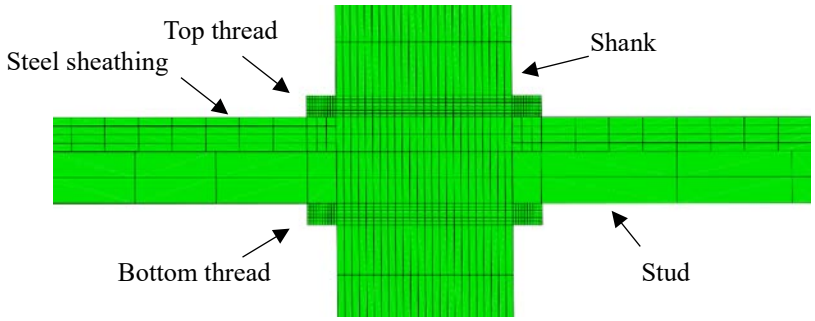

Fig. 9 Details of screw connections

The mesh densities in the vicinity of screws were refined as a consequence of the deformation mainly originating from this area, as shown in Fig. 9. The trilinear stress–strain curves in Fig. 10, which were established from coupon tests carried out by Ye Jihong and Feng Ruoqiang et al. [15], were adopted for the steel and the screw. To improve computational efficiency, the material of screw shank was assumed as perfect elastic in specimens without distortion of shank.

To simulate the influence of initial imperfections such as initial screw titling and clearance among the screw, the steel sheathing and studs. The varied stiffness spring was used in the model, which was realized by a linkage unit connected the loading point RP-2 with another point RP-1 coupled with the flanges of studs as a rigid body. The end of steel sheathing was fixed as shown in Fig. 8.

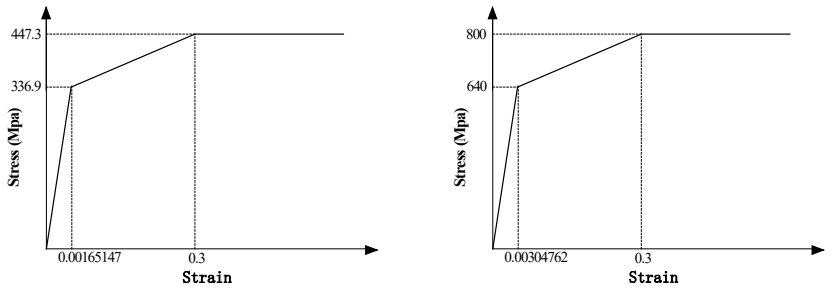

(a) Steel (b) Screw

Fig. 10 The trilinear stress–strain curves of materials

4.2 Failure mechanisms of models

Two failure modes were observed from models: the screws pulled out and sheared off. Most of specimens with the failure mode of screw pullout exhibited screw tilting, sheathing bearing and studs bearing, as shown in Fig. 11(a-c). The von Mises stress distribution showed that yielding occurs in areas around the screw hole in direct contact with the screw shank and the screw thread in contact with the studs.

Specimen 150-1.2P25MTS12G12-4.8 exhibited screw shearing in combination with screw tilting, sheathing bearing and studs bearing. Stress concentration was located on the screw shank in contact with sheathing, as shown in Fig. 11(d). Moreover, the stud occurred relative moving, which resulted the diameter of the middle shank was smaller. The failure mechanisms of models tallied with the tests.

4.3 Shear carrying capacity

The load–displacement curves of connections by modeling were the same as the test results, as shown in Fig. 12. However, compared with the test, the stiffness of slopes before the peak is larger and the relative displacements corresponding to peak loads were smaller by simulation. This is because the tearing of steel is not considered in the models, which is also the reason why there is no drop in the curve of specimen 150-1.2P25MTS12G12-4.8.

Table 4 shows the contrast of peak loads between modeling and tests with the relative error not exceeding 12.9%, which indicated the effectiveness of the finite element models.

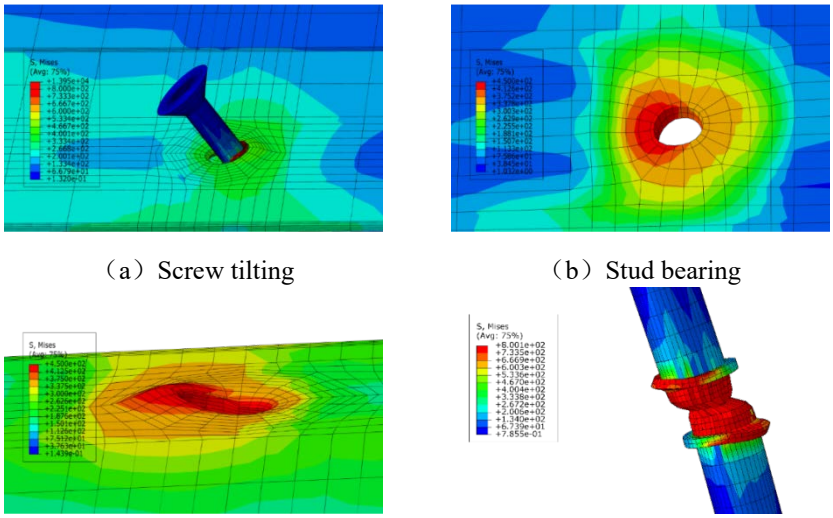

（a）Screw tilting （b）Stud bearing

（c）Steel sheathing bearing （d）Screw shearing

Fig. 11 Failure mechanisms of modeling

5. Conclusion

An experimental study of screw connections under monotonic loads in CFS shear walls sheathed with steel sheet for the base layer combined with gypsum wallboards for the face layer is described. Factors such as screw end distance, screw edge distance, screw diameter space, sheathing thickness and stud thickness are considered. A finite element modeling on screw connections is carried out with geometric non-linearity and material non-linearity, which shows a good agreement with test results.

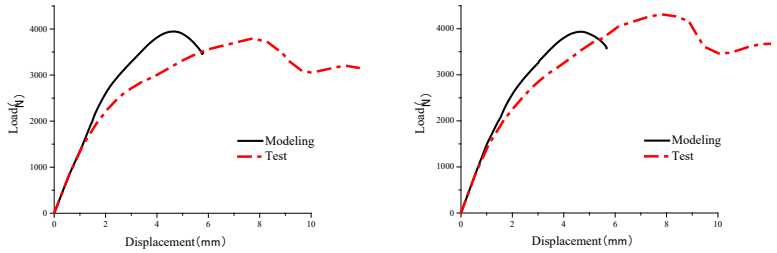

(a) 150-1.2P15MTS8G12-4.8 (b) 150-1.2P20MTS8G12-4.8

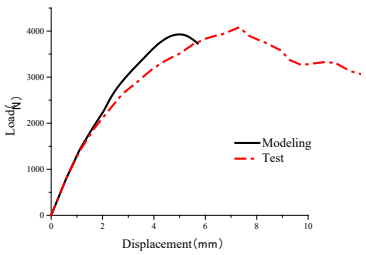

(c) 150-1.2P25MTS8G12-4.8-2G2S

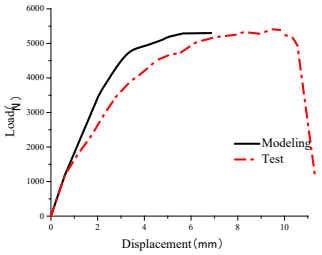

(d) 150-1.2P25MTS12G12-4.8

Fig. 12 Typical load–displacement curves of connections

Table 4
The contrast of peak loads between modeling and tests

Specimens	F_m（N）	F_e（N）	η
150-1.2P15MTS8G12-4.8	3945.2	3902.1	1.1%
150-1.2P20MTS8G12-4.8	3935.4	4364.0	-9.8%
150-1.2P25MTS8G12-4.8	3927.3	4222.4	-6.9%
100-1.2P25MTS8G12-4.8	3882.8	3964.1	-2.1%
200-1.2P25MTS8G12-4.8	3891.1	4018.9	-3.1%
150-0.9P25MTS8G12-4.8	3700.2	4026.7	-8.1%
150-2.5P25MTS8G12-4.8	4991.1	4421.3	12.9%
150-1.2P25MTS8G12-4.2	3771.5	4107.6	-8.1%
150-1.2P25MTS8G12-5.5	4322.2	4480.7	-3.5%
150-1.2P25MTS12G12-4.8	5288.5	5611.9	-5.7%

$\eta = \frac{Fm-Fe}{Fe} \times 100\%$;$F_m$ is the peak load in modeling and F_e is the average peak load in tests.

The conclusions of this study are summarized as follows:

(1) The failure of screw connections manifests a combination of several destruction phenomena included screws tilting, screw shearing, sheathing bearing, stud bearing and sheathing tearing. Specimens exhibit ductile failure expect specimens with 1.2 mm steel sheathing, which presents brittle failure due to screw shearing.

(2) Screw edge distance over 15 mm, screw end distance over 15 mm, screw spacing over 100 mm and gypsum wallboards thickness have little effect on shear capacities of screw connections. Increase of screw diameter, steel sheathing thickness and stud thickness can improve the shear capacities of screw connections.

(3) The finite element modeling have a good agreement in peak loads and failure modes with tests, whereas the stiffness of slopes before the peak and

the relative displacements corresponding to peak loads are inconsistent with the tests results, without considering steel tearing in simulation.

References

[1] Ye J, Wang X, Jia H, et al. Cyclic performance of cold-formed steel shear walls sheathed with double-layer wallboards on both sides[J]. Thin-Walled Structures, 2015, 92: 146-159.

[2] Code of design on building fire protection and prevention. Beijing, China: GB 50016-2006, China Planning Press; 2006 [in Chinese].

[3] Chen W, Ye J, Bai Y, et al. Full-scale fire experiments on load-bearing cold-formed steel walls lined with different panels[J]. Journal of Constructional Steel Research, 2012, 79: 242-254.

[4] Balh N, Dabreo J, Ong-Tone C, et al. Design of steel sheathed cold-formed steel framed shear walls[J]. Thin-Walled Structures, 2014, 75(2):76-86.

[5] Niari S E, Rafezy B, Abedi K. Seismic behavior of steel sheathed cold-formed steel shear wall: Experimental investigation and numerical modeling[J]. Thin-Walled Structures, 2015, 96: 337-347.

[6] Mohebbi S, Mirghaderi R, Farahbod F, et al. Experimental work on single and double-sided steel sheathed cold-formed steel shear walls for seismic actions[J]. Thin-Walled Structures, 2015, 91:50-62.

[7] Rogers C A, Hancock G J. Failure Modes of Bolted-Sheet-Steel Connections Loaded in Shear[J]. Journal of Structural Engineering, 2013, 126(3):288-296.

[8] L. Fiorino, G. Della Corte, R. Landolfo. Experimental tests on typical screw connections for cold-formed steel housing[J]. Engineering Structures, 2007, 29(8): 1761-1773.

[9] Nithyadharan M, Kalyanaraman V. Experimental study of screw connections in CFS-calcium silicate board wall panels[J]. Thin-Walled Structures, 2011, 49(6): 724-731.

[10] Wei Lu, Zhongcheng Ma, Pentti Mäkeläinen, Jyri Outinen. Behaviour of shear connectors in cold-formed steel sheeting at ambient and elevated temperatures[J]. Thin-Walled Structures, 2012, 61: 229-238.

[11] Fan L, Rondal J, Cescotto S. Finite element modelling of single lap screw connections in steel sheeting under static shear[J]. Thin-Walled Structures, 1997, 27(2):165-185.

[12] Chung K F, Ip K H. Finite element modeling of bolted connections between cold-formed steel strips and hot rolled steel plates under static shear loading[J]. Engineering Structures, 2000, 22(10):1271-1284.

[13] R. Park, Evaluation of ductility of structures and structural assemblages from laboratory testing, Bull. N Z Natl. Soc. Earthq. Eng. 22 (3) (1989) 155–166.

[14] ABAQUS/Standard, Version 6.11.

[15] Ye Jihong, Feng Ruoqiang et al. Seismic Technology Handbook of light steel structure building in villages and towns[M]. Nanjing: Southeast University Press，2013, 23.